

Correlation Sketches for Approximate Join-Correlation Queries

Aécio Santos¹, Aline Bessa¹, Fernando Chirigati², Christopher Musco¹, Juliana Freire¹

¹New York University

{aecio.santos,aline.bessa,cmusco,juliana.freire}@nyu.edu

²Springer Nature

fernando.chirigati@us.nature.com

ABSTRACT

The increasing availability of structured datasets, from Web tables and open-data portals to enterprise data, opens up opportunities to enrich analytics and improve machine learning models through relational data augmentation. In this paper, we introduce a new class of data augmentation queries: *join-correlation queries*. Given a column Q and a join column K_Q from a query table \mathcal{T}_Q , retrieve tables \mathcal{T}_X in a dataset collection such that \mathcal{T}_X is joinable with \mathcal{T}_Q on K_Q and there is a column $C \in \mathcal{T}_X$ such that Q is correlated with C . A naïve approach to evaluate these queries, which first finds joinable tables and then explicitly joins and computes correlations between Q and all columns of the discovered tables, is prohibitively expensive. To efficiently support correlated column discovery, we 1) propose a sketching method that enables the construction of an index for a large number of tables and that provides accurate estimates for join-correlation queries, and 2) explore different scoring strategies that effectively rank the query results based on how well the columns are correlated with the query. We carry out a detailed experimental evaluation, using both synthetic and real data, which shows that our sketches attain high accuracy and the scoring strategies lead to high-quality rankings.

CCS CONCEPTS

• Information systems → Data management systems.

ACM Reference Format:

Aécio Santos, Aline Bessa, Fernando Chirigati, Christopher Musco, Juliana Freire. 2021. Correlation Sketches for Approximate Join-Correlation Queries. In *Proceedings of the 2021 International Conference on Management of Data (SIGMOD '21)*, June 20–25, 2021, Virtual Event, China. ACM, New York, NY, USA, 14 pages. <https://doi.org/10.1145/3448016.3458456>

1 INTRODUCTION

The increasing availability of structured datasets, from Web tables [19, 51] and open-data portals (see e.g., [58, 59, 74]) to enterprise data, opens up opportunities to enrich analytics and improve machine learning models through *relational data augmentation*. The challenge lies in finding relevant datasets for a given task. In this paper, we explore a new class of data search queries that retrieve

related datasets by uncovering correlations between numerical columns in unjoined datasets. Consider the following examples.

Example 1: Explaining Traffic Fatalities. Based on the observation that there is a relationship between high traffic speed and the number of fatalities, the City of New York, as part of the Vision Zero initiative [57], reduced the speed limit on its streets from 30 to 25 miles per hour. While the lower speed limit was partially effective, fatalities were still high and there was a need to understand why. Analysts hypothesized that an increased number of bikes and the weather can also lead to more traffic fatalities. By examining datasets published in NYC Open Data [58], they validated their hypotheses: from CitiBike data, they found that when there are more active bikes, there are more accidents; and they also observed that high precipitation is correlated with a larger number of accidents.

Example 2: Improving Taxi Demand Models. A data scientist at the NYC Taxi & Limousine Commission created a model to predict taxi demand using a dataset that contains historical data about taxi trips and their associated pick-up times and location zip codes. To improve the model, she had to find additional features that can influence taxi demand. Domain experts suggested a set of indicators for her to examine, including weather, major events, and holidays. She obtained the relevant datasets and observed a substantial reduction in the root mean squared error after augmenting the training data.

In both examples, the analysts knew which datasets they needed and where to find them. Often, this is not the case: finding relevant data is a difficult and time-consuming task [36]. On the Web, data are distributed over many sites and repositories, and in enterprises they are stored in a plethora of systems and databases. As a point of reference, internal research at Lyft has found that their data scientists spend 25% of their time on data discovery – they only spend more time (40%) on model development and deployment [39].

The interest in data search is growing in both industry and academia. In enterprises, there is an increasing number of “data catalog” systems [4, 39, 50, 73] that support data search across multiple systems and data lakes. This market is projected to grow from USD 528.3 million in 2019 to USD 5.46 billion in 2027 [40]. Dataset search engines that provide search over datasets on the Web [17] are also becoming available. While these systems fill important gaps in the data discovery space, they often have limited query capabilities, supporting only queries over dataset metadata.

Recent research proposes methods that support dataset-oriented queries to retrieve datasets that can be concatenated [56] or joined with a given dataset [20, 77, 84]. However, neither supports the discovery tasks illustrated in the examples above. Specifically, these tasks demand a new type of augmentation query to *find datasets that can be joined with and that also contains attributes that are correlated with those of a given query dataset*.

Permission to make digital or hard copies of all or part of this work for personal or classroom use is granted without fee provided that copies are not made or distributed for profit or commercial advantage and that copies bear this notice and the full citation on the first page. Copyrights for components of this work owned by others than ACM must be honored. Abstracting with credit is permitted. To copy otherwise, or republish, to post on servers or to redistribute to lists, requires prior specific permission and/or a fee. Request permissions from permissions@acm.org.

SIGMOD '21, June 20–25, 2021, Virtual Event, China

© 2021 Association for Computing Machinery.

ACM ISBN 978-1-4503-8343-1/21/06...\$15.00

<https://doi.org/10.1145/3448016.3458456>

Discovering Correlated Datasets. Augmentation queries over large dataset collections can enable analysts to uncover previously unknown relationships that lead to new hypotheses. In Example 1, to explore the question “What causes traffic fatalities?”, the analyst could search the NYC Open Data [58] repository for data *related* to the traffic fatalities dataset, which contains the total number of daily fatalities for each zip code; and in Example 2, she could search for data related to the taxi demand dataset, which consists of the total number of hourly pickups per zip code.

For both examples, methods devised to find joinable tables [20, 84, 85] would find relevant results among over 2,000+ datasets in NYC Open Data, but they would find *too many*. Specifically, these methods find columns that have a large overlap with the input dataset, so they would return all datasets that contain a column with zip codes in NYC – most of which are not helpful to the users’ information needs. For the examples above, further filtering is needed. To express their information need more precisely, analysts would benefit from asking *join-correlation queries*.

Definition 1 (Join-Correlation Query). *Given a column Q and a join column K_Q from a query table \mathcal{T}_Q , a join-correlation query finds tables \mathcal{T}_X in a dataset collection such that \mathcal{T}_X is joinable with \mathcal{T}_Q on K_Q and there is a column $C \in \mathcal{T}_X$ such that Q is correlated with C .*

In our first example, the analysts could issue a query to retrieve datasets that join with the traffic fatalities dataset and that also contain a column that correlates with the actual number of fatalities; in the second, the data scientist could search for datasets that join with the taxi demand dataset and that contain a column that correlates with the actual taxi demand.

The key challenge in evaluating *join-correlation queries* is how to do so efficiently. One approach is to first find joinable tables, and then to explicitly compute correlations between Q and all columns of the discovered tables using, for instance, the Pearson’s correlation coefficient for linear relationships, or the Spearman’s rank correlation coefficient to capture non-linear relationships [61]. However, this approach requires the joinable datasets returned to be downloaded and joined with the query table. When these tables are large, they may not fit in memory and the cost of executing join operations can be prohibitive. Furthermore, some correlation measures are expensive to compute, e.g., to compute Spearman’s correlation the data must first be sorted. This problem is compounded for queries that return a large number of datasets and require many joins and correlation computations to be performed. As a point of comparison, joining a dataset on taxi pickups (approximately 1GB) with a dataset on precipitation (approximately 3MB) took about 29 seconds and computing the Spearman’s coefficient between the numbers of pickups and precipitation levels in the resulting joined dataset took about 5 seconds (on a Intel Core i5 2.4GHz CPU).

Our Approach: Ranking Datasets via Correlation Estimates. To reduce the evaluation cost of join-correlation queries, as an alternative to using the entire data, we investigate the use of data synopses to estimate the results. Data-intensive algorithms can often be optimized by reducing the size of the input data with sampling techniques [26], at the cost of obtaining approximate results. In our setting, however, naïvely sampling data to estimate correlations does not work: it is not possible to sample columns to estimate

the correlation without first executing the join. To support the *efficient discovery of correlated columns from distinct datasets at scale*, we propose a sketching method for *estimating correlations between columns from unjoined datasets* based on column synopses, namely *Correlation Sketches*. These synopses are constructed using only data from individual columns, and thus they can be *pre-computed and indexed* to support discovery of joinable datasets and *fast correlation estimation* at query time.

Our method constructs a synopsis $L_{\langle K_X, X \rangle}$ for any given pair of columns $\langle K_X, X \rangle$ that belongs to a table \mathcal{T}_X , where K_X is a categorical column and X is a numerical column. A pair of synopses $L_{\langle K_X, X \rangle}$ and $L_{\langle K_Y, Y \rangle}$ (for tables \mathcal{T}_X and \mathcal{T}_Y respectively) can be used to estimate the correlation between the numerical columns $X_{X \rightarrow Y}$ and $Y_{X \rightarrow Y}$, generated *after* joining tables \mathcal{T}_X and \mathcal{T}_Y on columns K_X and K_Y . Note that \mathcal{T}_X and \mathcal{T}_Y are heterogeneous and need not have the same join keys or the same number of rows. As such, our sketching method enables the construction of an index for a large number of tables that can be used to support *both* joinability queries and to estimate the correlation between a query column and indexed columns.

Our sketching method builds upon and extends state-of-the-art hashing techniques [5, 8, 9, 45, 77]. In particular, we prove that our sketches can reconstruct a uniform random sample of the paired columns $X_{X \rightarrow Y}$ and $Y_{X \rightarrow Y}$. This leads to an important property: besides correlations, our sketching approach can handle *any* statistic that can be estimated from random samples (e.g., entropy and mutual information). While other statistics are out of the scope of this paper, we demonstrate the flexibility of our method by using it to estimate a variety of different correlation coefficients.

We show both theoretically and experimentally that our approach is effective and provides accurate estimates for correlation. Moreover, our analysis provides mathematical tools for dealing with approximation errors typical of sketching algorithms. For join-correlation queries, these errors may lead to false positives: columns are returned which seem more correlated, based on the sketch, than they actually are. This problem is an issue for queries over large dataset collections, as there can be many false positives, simply by chance. To address this issue, we derive sub-sample confidence interval bounds to estimate approximation errors. Our bounds are based on simple columns statistics like sample size and data range and, in contrast to prior work [7, 12, 13], do not rely on distributional assumptions. We use these bounds to design a set of scoring functions that rank datasets based on both their estimated correlation with a query dataset, and on our confidence in that estimate.

We evaluate our method experimentally using both synthetic and real-world datasets. A comparison of the estimates produced by *Correlation Sketches* with the actual correlation values shows that it derives accurate estimates. In addition, we assess the effectiveness of different ranking functions that leverage *Correlation Sketches*, and show that they improve ranking performance up to 193% in terms of mean average precision when compared to a scoring scheme based on overlap size, commonly used for joinability queries [20, 84, 85].

Contributions. We introduce *join-correlation queries*, a new class of queries to find correlated datasets within a collection of disconnected tables, and propose new methods to efficiently support such queries over large dataset collections. To the best of our knowledge,

ours is the first work that addresses this problem. Our contributions can be summarized as follows:

- We propose *Correlation Sketches*, a new sketch that simultaneously summarizes information about joinability and correlation, allowing the estimation of different correlations measures between columns of unjoined datasets (Section 3).
- We derive new correlation confidence interval bounds that allow us to measure the risk of estimation errors. These bounds serve as the basis for the design of scoring functions that use our sketches to rank the discovered columns (Section 4).
- We perform an extensive experimental evaluation of our method and show that: *Correlation Sketches* estimates correlations with good accuracy in both synthetic and real data for different correlation measures; and the scoring functions we propose are effective and derive high-quality rankings (Section 5).

2 PRELIMINARIES

Our approach extends existing hashing-based methods proposed for cardinality estimation to the join-correlation query problem. We describe these methods below. For more details, we refer the reader to Section 6 and to a comprehensive survey on the topic [26]. We also review the literature on correlation estimation and discuss the properties of correlation estimators that we use in this paper.

2.1 Cardinality Estimation via Sketches

Estimating Distinct Values. The problem of determining the number of distinct values (DV) in a dataset has been extensively studied [18, 46, 60] Since computing the *exact* number of distinct elements is expensive, approximate methods have been proposed that can scale to massive collections of datasets. Effective approaches for DV estimation rely on hashing techniques, require a single pass through the data, and use a bounded amount of memory [42].

Let h_u be a hash function that maps distinct values randomly and uniformly to the unit interval $[0, 1]$, and D be the number of distinct elements in a dataset. The key idea behind DV estimators is that, if we use h_u to map elements to the unit interval and the number of distinct elements in a dataset is large (i.e., $D \gg 1$), then the expected distance between any two neighboring points in the unit interval is $1/(D+1) \approx 1/D$, and the expected value of the k^{th} smallest point, $U(k)$, is estimated with $\mathbb{E}[U(k)] \approx \sum_{j=1}^k (1/D) = k/D$. Thus, the number of distinct values in the dataset can be approximated by $D \approx k/\mathbb{E}[U(k)]$. The simplest estimator of $\mathbb{E}[U(k)]$ is $U(k)$ itself, yielding the basic estimator: $\hat{D}_k^{BE} = k/U(k)$.

Based on this idea, algorithms and methods for building synopses have been developed to estimate set cardinality [8]. An example is the popular k *Minimum Values* (KMV) synopsis (also known as bottom- k sketches), introduced by Bar-Yossef et al. [5]. Concretely, a KMV synopsis of a set X comprises the k minimum hash values of the elements of X , generated by a hash function h_u mapping to $[0, 1]$. To estimate the number of distinct elements $|X|$, one can use this synopsis and a DV estimator, such as \hat{D}_k^{BE} . Alternatively, an improved DV estimator proposed by Beyer et al. [9] can be used. Their estimator, given by $\hat{D}_k^{UB} = (k-1)/U(k)$, is unbiased, has a lower mean squared error, and has the minimal possible variance of any DV estimator when there are many distinct values and the synopsis size is large.

Cardinality Estimation under Set Operations. Beyer et al. [9] also considered how multiple KMV synopses, created independently, can be combined to estimate the cardinality of sets that result from multi-set operations (e.g., union, intersection, and difference). As an example, consider a set X composed of two partitions X_A and X_B , i.e., $X = X_A \cup X_B$. Next, let L_A and L_B be the KMV synopses of sets X_A and X_B , with sizes k_A and k_B respectively. We can combine L_A and L_B to build a valid KMV synopsis $L = L_A \oplus L_B$, where \oplus is an operator for combining two KMV synopses. L represents the set comprising the k smallest values in $L_A \cup L_B$, where $k = \min(k_A, k_B)$. To estimate the number of distinct elements D_U in the union $X_A \cup X_B$, we can directly use estimator \hat{D}_k^{UB} on the synopsis L . To estimate the number of distinct values D_\cap in the intersection $X_A \cap X_B$, we must first compute the number of common distinct hashes in L_A and L_B (i.e., $K_\cap = |\{v \in L : v \in L_A \cap L_B\}|$). Then, we can estimate D_\cap as:

$$\widehat{D}_\cap = \frac{K_\cap k - 1}{k U(k)} \quad (1)$$

2.2 Correlation Estimation

The problem of measuring dependence between a pair of vectors has been studied for over a century [62], and new correlation measures continue to be developed [3, 67]. Pearson’s correlation coefficient is one of the oldest and most widely used correlation measures [61]. While our methods can be used to estimate any measure of correlation, we use Pearson’s as our main motivating example.

When applied to a population, Pearson’s correlation coefficient is usually referred to as ρ [61]. For a pair of random variables $\langle X, Y \rangle$, the coefficient is defined as:

$$\rho_{XY} = \frac{\mathbb{E}[(X - \mu_X)(Y - \mu_Y)]}{\sigma_X \sigma_Y} \quad (2)$$

where σ_X (resp. σ_Y) is the standard deviation of the random variable X (resp. Y), and μ_X (resp. μ_Y) is the mean of X (resp. Y). ρ_{XY} can be estimated with a finite sample from distributions X and Y using what is usually referred to as Pearson’s sample correlation (r):

$$r_{XY} = \frac{\sum_{i=1}^n (x_i - \bar{x})(y_i - \bar{y})}{\sqrt{\sum_{i=1}^n (x_i - \bar{x})^2} \sqrt{\sum_{i=1}^n (y_i - \bar{y})^2}} \quad (3)$$

Above n is the sample size, x_i and y_i are individual samples, and \bar{x} and \bar{y} are, respectively, the means of the sub-samples of X and Y .

There is a lot of prior work on understanding the accuracy of sample correlation estimators, but these works typically make strong data assumptions. When data follows a bivariate normal distribution, the sampling distribution of r is asymptotically normal and centered around ρ [64]. For a finite sample of size n , the variance of r is known to depend both on n and on the underlying population correlation ρ [65]:

$$\text{Var}(r) = \frac{(1 - \rho^2)^2}{n - 1} \quad (4)$$

When data is not normally distributed (as is often the case in practice), less is known. Nevertheless, there has been an increasing interest in the non-normal setting in recent years [10–13, 30, 44, 79]. Yuan and Bentler [79, 80] show asymptotically that the standard deviation of the sample estimator r depends on the joint fourth-order moments, or kurtoses, of the variables. In agreement, empirical simulations confirm that the presence of a high excess kurtosis can lead to increased bias and estimator errors [12, 30].

\mathcal{T}_X		\mathcal{T}_Y		$\mathcal{T}_{X \bowtie Y}$		
K_X	X	K_Y	Y	$K_{X \bowtie Y}$	$X_{X \bowtie Y}$	$Y_{X \bowtie Y}$
2021-01	6.0	2021-01	5.5	2021-04	3.0	4.0
2021-02	4.0	2021-01	4.5	2021-03	2.0	2.5
2021-03	2.0	2021-02	3.9	2021-02	4.0	3.0
2021-04	3.0	2021-02	2.0	2021-01	6.0	5.0
2021-05	0.5	2021-03	4.0			
2021-06	4.0	2021-03	1.0			
2021-07	2.0	2021-04	4.0			

Figure 1: Table $\mathcal{T}_{X \bowtie Y}$ is the join of the input tables \mathcal{T}_X and \mathcal{T}_Y , aggregated using the mean function. Correlation Sketches efficiently reconstructs a sample of the table $\mathcal{T}_{X \bowtie Y}$ to estimate correlation between the columns $X_{X \bowtie Y}$ and $Y_{X \bowtie Y}$, without computing the full join.

Robustness and Alternative Correlations. One challenge in obtaining finite sample accuracy bounds, as we do in Section 4.3, is that Pearson’s correlation coefficient is known to be sensitive to outliers. In fact, it has been shown that a single sample (x_i, y_i) can have an unbounded effect on the correlation and can potentially lead to catastrophic estimation errors [32]. This fact has spurred the development of correlation estimators that are robust against outliers and distribution contamination [32, 64]. However, these robust estimators are less efficient than r , i.e., require larger sample sizes. We refer the reader to [64] for an extensive review of robust correlation estimators. Resampling-based approaches such as bootstrapping [34] can also be used to reduce error in estimating Pearson’s correlation, especially at small sample sizes [12]. These approaches, however, have a much higher computational cost [12].

Alternative correlation measures, such as the Spearman’s rank correlation coefficient [61], and data distribution transformations, such as the Rank-based Inverse Normal (RIN) [11, 14], may be more effective than Pearson for highly non-normal data [12]. However, they have different semantics from Pearson’s (e.g., they capture non-linear relationships), and thus the choice of correlation measure depends on the user’s application. All of these correlations can be estimated with our approach, and we experimentally show that the accuracy of our estimates for these estimators are similar in the data collections we have considered (Section 5).

3 ESTIMATING JOIN-CORRELATION

Before presenting *Correlation Sketches*, we introduce notation and formally define the join-correlation estimation problem. Consider a query table \mathcal{T}_X composed of a categorical column K_X and a numerical column X , and a table \mathcal{T}_Y in a dataset collection containing a categorical column K_Y and a numerical column Y (we discuss below how multi-column tables are handled). Columns K_X and K_Y are the join attributes, i.e., $\mathcal{T}_{X \bowtie Y} = \pi_{k, x_k, y_k}(\mathcal{T}_X \bowtie_{K_X=K_Y} \mathcal{T}_Y) = \{\langle k, x_k, y_k \rangle : k \in K_X \cap K_Y\}$. We denote by x_k and y_k the numerical values of X and Y (respectively) associated with the row identified by key k . This is illustrated in Figure 1.

Definition 2 (Join-Correlation Estimation). *Given two tables \mathcal{T}_X and \mathcal{T}_Y , we aim to efficiently estimate the correlation $r_{X \bowtie Y}$ of the numerical attributes $X_{X \bowtie Y}$ and $Y_{X \bowtie Y}$ in $\mathcal{T}_{X \bowtie Y}$ without having to compute the join and aggregations for \mathcal{T}_X and \mathcal{T}_Y .*

One approach to estimate $r_{X \bowtie Y}$ is to use data sketches instead of the full datasets. To do so, we can build synopses $L_{(K_X, X)}$ and $L_{(K_Y, Y)}$ that serve as summaries of (K_X, X) and (K_Y, Y) respectively. However, naive approaches do not yield useful summaries.

$L_{(K_X, X)}$			$L_{(K_Y, Y)}$			$L_{(X \bowtie Y)}$		
$h(k)$	$h_u(k)$	x_k	$h(k)$	$h_u(k)$	y_k	$h(k)$	x_k	y_k
bac52e98	0.48	2.0	16dab449	0.34	2.5	16dab449	2.0	2.5
16dab449	0.34	2.0	bd5a7c1f	0.89	3.0	26f79756	3.0	4.0
26f79756	0.47	3.0	26f79756	0.47	4.0	4da33cf5	6.0	5.0
4da33cf5	0.34	6.0	4da33cf5	0.34	5.0			

Figure 2: The tables $L_{(K_X, X)}$ and $L_{(K_Y, Y)}$ represent correlation sketches for the tables \mathcal{T}_X and \mathcal{T}_Y , for sketch size $n = 3$ and mean aggregation. While we explicitly show the column $h_u(k)$ for illustrative purposes, it does not need to be stored as it can be easily computed from $h(k)$.

Limitations of Random Sampling. Consider, for example, two numerical vectors of size n , S_X and S_Y , randomly sampled from the numerical columns $X \in \mathcal{T}_X$ and $Y \in \mathcal{T}_Y$, respectively. The correlation between S_X and S_Y is not a valid estimate of the correlation between $X_{X \bowtie Y}$ and $Y_{X \bowtie Y}$ because the pairs $\langle x \in S_X, y \in S_Y \rangle$ are not aligned. By sampling directly from X and Y , we lose information on what keys are associated with what numerical values, which is necessary to align pairs $\langle x_k, y_k \rangle$. Another alternative would be to include the keys by randomly sampling rows from original tables \mathcal{T}_X and \mathcal{T}_Y , and then joining the row samples. However, since the final set of keys $k \in K_{X \bowtie Y}$ depends on input columns $K_X \in \mathcal{T}_X$ and $K_Y \in \mathcal{T}_Y$, it is unlikely that the keys selected from K_X and contained in $K_{X \bowtie Y}$ will also be selected from K_Y . We discuss this issue more formally in the next subsection.

3.1 Correlation Sketches

Correlation Sketches address the limitations of naive approaches by *enabling the reconstruction of a uniform random sample of the joined table*. Our method uses hashing techniques to carefully select a small sample of tuples $\langle k, x_k \rangle$ from a table $\mathcal{T}_X = \langle K_X, X \rangle$, that is used to build a sketch which enables data from different tables to be aligned and correlations to be estimated.

Sketch Construction. We use two different hashing functions to create the sketch $L_{(K_X, X)}$ for table \mathcal{T}_X . The first one, h , is a collision-free hash function that randomly and uniformly maps key values $k \in K_X$ into distinct integers. Given that these integers $h(k)$ are unique, they are used as the tuple identifiers in sketch $L_{(K_X, X)}$. Next, we use hashing function h_u to map integers $h(k)$ to real numbers in the range $[0, 1]$, uniformly at random. The function h_u plays a key role in the selection of the n tuples that compose the sketch $L_{(K_X, X)}$: the tuples that correspond to the n smallest h_u values are the ones included in the sketch. More formally, we select n samples of pairs $\langle h(k), x_k \rangle$ with minimum values of $h_u(k)$, i.e., $L_{(K_X, X)} = \{\langle h(k), x_k \rangle : k \in \min(k, h_u(k))\}$, where \min is a function that returns a set containing the keys k with the n smallest values of $h_u(k)$. To illustrate this, consider the example table \mathcal{T}_X in Figure 1. To build a correlation sketch, we apply the hashing functions to each one of the keys $k \in K_X$ and then select the n tuples associated with the smallest hashed values, which are used to create the *correlation sketch* $L_{(K_X, X)}$ in Figure 2.

Once these sketches are created (independently) for separate tables, they are used to estimate correlation by computing a *joined sketch* $L_{X \bowtie Y}$, also illustrated in Figure 2. $L_{X \bowtie Y}$ has a row for every key k that appears in both $L_{(K_X, X)}$ and $L_{(K_Y, Y)}$. As we argue in Theorem 1, this table contains a uniform random sample of paired numerical values from $\mathcal{T}_{X \bowtie Y}$, so it can be used directly to estimate correlation or any other statistic over $\mathcal{T}_{X \bowtie Y}$.

The accuracy of an estimate, however, depends on the size of this sample being large, i.e., on $L_{X \mapsto Y}$ having many rows. The key idea behind our method is that, by selecting samples using h_u , we introduce dependence that increases the probability of $L_{\langle K_X, X \rangle}$ and $L_{\langle K_Y, Y \rangle}$ including the same keys [45]. To see this, consider an extreme example where both K_X and K_Y have the same set of N distinct keys. Suppose that n key-value tuples $\langle k, x_k \rangle$ are included in $L_{\langle K_X, X \rangle}$ uniformly at random (without hashing), and n are also included in $L_{\langle K_Y, Y \rangle}$, independently and uniformly at random. If a key k is included in $L_{\langle K_X, X \rangle}$, the probability that it also appears in $L_{\langle K_Y, Y \rangle}$ is n/N . Thus, the expected number of rows in $L_{X \mapsto Y}$ is n^2/N , vanishingly small when the sketch size n is much smaller than N . With little or no key overlap, we have no way of effectively estimating correlation from $L_{X \mapsto Y}$. On the other hand, when the inclusion is determined by the values of $h_u(k)$, the events become dependent: if k is included in $L_{\langle K_X, X \rangle}$, k must also be included in $L_{\langle K_Y, Y \rangle}$. In this case, the number rows in $L_{X \mapsto Y}$ increases to n , the maximum number possible. In a less extreme case where K_X and K_Y do not have the exact same keys, the expected number of keys included in both sketches will depend on the Jaccard similarity between the key sets, but in any case, will be much larger than the n^2/N obtained by uniform random sampling.

Note that the use of a hashing function such as h_u to introduce dependence is not a new idea – it has been used in many algorithms [8, 28, 45, 71, 77]. Part of our contribution lies in the combination of h_u with another function h to generate tuple identifiers that *allow the alignment of paired data samples at estimation time*. Correlation Sketches contains both the n minimum hashed values $h(k)$ and their corresponding numerical values x_k from column X . By keeping the hash of the key, it is possible to align the numerical values with values in other tables that are associated with the same key, and by storing the numerical values, we can estimate the correlations between the numeric columns.

Handling Repeated Keys. The process described above assumes that the keys uniquely identify each row in a table. However, real-world data often contain repeated categorical values (as in column K_Y in Figure 1). In such cases, there is a set of values associated with each distinct key k . For instance, in Figure 1, the set of values $\{5.5, 4.5\}$ is associated with the key “2021-01”. Because correlation is only defined for sets of paired values, downstream applications that use correlation typically aggregate the numeric values associated with a key into a single number. This can be done by applying a user-defined function (e.g., *mean, sum, maximum, minimum, first, last*) to perform the aggregation before computing the correlation. In Figure 1, the column $Y_{X \mapsto Y}$ contains the aggregated values of Y using the *mean* function after the join between \mathcal{T}_X and \mathcal{T}_Y .

Repeated keys can be handled during sketch construction: whenever a key k that already exists in the set of hashed minimum values is found again at time t , an aggregate function f can be applied to compute the value for time t by aggregating the existing x_k^{t-1} with the new incoming x_k , i.e., $x_k^t = f(x_k, x_k^{t-1})$. As long as the aggregation can be computed in a streaming fashion, the synopsis can also be computed with a single pass over the data. $L_{\langle K_Y, Y \rangle}$ in Figure 2 shows a sketch constructed from table \mathcal{T}_Y in Figure 1, using *mean* as the aggregate function f .

Note that the choice of function affects the semantics of the data, thus this selection must be made by taking into account the requirements of the downstream application that makes use of the sketches. Nonetheless, our synopsis is agnostic to such aggregations, and can easily be extended to take as input one or more functions.

Sketches for Multi-Column Tables. For simplicity, we described how to build sketches from a binary table, but it is trivial to extend to process to multi-column tables. For example, if a table contains multiple columns, $\mathcal{T}_{XZ} = \{K_{XZ}, X, Z\}$, the correlation sketch could be extended to $L_{\langle K_{XZ}, X, Z \rangle} = \{\langle h(k), x_k, z_k \rangle : k \in \min(k, h_u(k))\}$. Alternatively, one could simply build one sketch for each pair of keys and numeric columns, e.g., $\langle K_X, X \rangle$ and $\langle K_Z, Z \rangle$.

3.2 Estimating Join-Correlation

An important property of *Correlation Sketches* is that it enables the construction of a *uniform random sample* of the join $\mathcal{T}_{X \mapsto Y}$. This can be formally stated as (proof is deferred to the appendix):

THEOREM 1. *The set of paired numeric values $\langle x_k, y_k \rangle \in L_{X \mapsto Y}$ is a uniform random sample of the set of paired numeric values $\langle x_k, y_k \rangle \in \mathcal{T}_{X \mapsto Y}$.*

Common measures of correlation, such as Pearson and Spearman, can be approximated with a sub-sample of data from those columns, as long as that sample is taken uniformly at random. Theorem 1 forms the basis of our algorithm for join-correlation estimation, which consists of two steps: (1) create the synopsis table $L_{X \mapsto Y}$ by performing a join between two synopses L_X and L_Y on their hashed keys $h(x)$ (as illustrated in Figure 2), and (2) apply *any* sample correlation estimator to the numerical data of $L_{X \mapsto Y}$ to estimate the correlation between columns X and Y in $\mathcal{T}_{X \mapsto Y}$.

3.3 Discussion

From Theorem 1, we know that correlation sketches provide a valid estimate of the correlation between any two data columns *after a join* – i.e., between $X_{X \mapsto Y}$ and $Y_{X \mapsto Y}$. While this estimate is often accurate, it is based on a sub-sample of data and inaccurate estimates are inevitable (see e.g., Figure 3). Of course, this will be true for any randomized estimator, not just our algorithm.

The variance of Correlation Sketches estimates depends on the correlation estimator used. In general, as we show in Section 5, correlation estimates converge to the true correlation when the sketch join sample size (i.e., the number of rows in $L_{\langle X \mapsto Y \rangle}$) increases. This sketch join size depends on multiple factors. First, there is a space-accuracy trade-off: as the number of minimum hash n increases, the probability of having larger join sizes also increases. The sketch join size also depends on the distribution of the join keys. Therefore, the hashing selection strategy used to include tuples in the synopsis affects the sketch intersection size, and ultimately it also affects the variance of correlation estimation.

The fixed-size sample selection strategy adopted in this paper is similar to the hashing strategy in [9], i.e., the sketch contains the n minimum values of $h_u(k)$. However, there is a wide range of possible hashing strategies with variable size [28, 77] that may have different accuracy-space trade-offs and could be used in Correlation Sketches. Exploring the effect of different selection strategies on join-correlation estimation is an open problem that we would like to explore in future work.

Another benefit of Correlation Sketches is that it retains all information contained in a KMV sketch [5, 9]. Therefore, it allows not only for the estimation of correlations associated to numerical columns, but it also enables the estimation of all statistics supported by the family of minimum-value sketches (e.g., cardinality, Jaccard containment, and similarity). These could be used, for example, to estimate the number of distinct elements in each individual column (K_X and K_Y), the containment of K_X in K_Y , and the size of the resulting join table $\mathcal{T}_{X \bowtie Y}$.

3.4 Implementation

We used the well-known 32-bits MurmurHash3 function to implement h , since it has been shown to perform similarly to truly random hashing functions [27]. For h_u , we used Fibonacci hashing [49], a simple multiplicative hashing function (also known as the *golden ratio multiplicative hashing*). To build the synopses, we implemented a tree-based algorithm similar to the one described in [9]. In summary, the algorithm performs one pass in the data while maintaining a tree that keeps the n tuples $\langle h(k), h_u(k), x_k \rangle$ with minimum $h_u(k)$ values. As we discuss in Section 5.3, we also implemented multiple correlation estimators.

4 RANKING CORRELATED COLUMNS

To query large dataset collections, we focus on a variation of join-correlation queries that retrieve the top- k results, which we define more formally as follows.

Definition 3 (Top- k Join-Correlation Query). *Given a column Q and a join column K_Q from a query table \mathcal{T}_Q , find the top- k tables \mathcal{T}_X in a dataset collection such that \mathcal{T}_X is joinable with \mathcal{T}_Q on K_Q and has the highest after-join correlations between a column $C \in \mathcal{T}_X$ and Q .*

Exact top- k join-correlation queries can be answered by finding all tables \mathcal{T}_X that are joinable on K_Q , performing a full join, and finally finding the tables that have the k greatest correlations. As we discussed, this is inefficient and does not scale when querying large dataset collections. Instead, we propose an efficient approach to compute approximate answers for these queries that uses Correlation Sketches to *rank the results based on correlation estimates*.

The possibility of error presents a challenge for answering approximate join-correlation queries. While searching for columns correlated with query column Q within a large collection of disconnected tables, there will typically be many more poorly-correlated columns than highly-correlated ones. In this “needle-in-a-haystack” setting, estimation errors will lead to many false positive results: inevitably some poorly-correlated columns will look far more correlated with Q than they actually are, even more correlated than the columns we aim to find. Therefore, simply ranking results based on the correlation estimates may eventually produce poor rankings. In the remainder of this section, we propose a framework for scoring columns that addresses this problem.

Another important aspect of an implementation of our method is query evaluation. While Correlation Sketches efficiently estimate join-correlations, a naïve approach that computes correlations for all possible column pairs can still be expensive for large collections. Computing correlations for all pairs, however, is not necessary: not all possible join keys have a high key overlap to yield useful joins. To efficiently answer top- k join-correlation queries we can

leverage efficient data structures and query processing algorithms for set overlap search. Recall that a sketch includes a set of pairs $\langle h(k), x_k \rangle$. Since $h(k)$ is a discrete value, we can leverage existing data structures for efficient querying such as inverted indexes available in off-the-shelf systems (e.g., PostgreSQL, Apache Lucene) and efficient query processing algorithms for set similarity search such as JOSIE [84], ppjoin+ [76], CRSI [70], and Lazo [20].

4.1 Ranking with Uncertain Estimates

To take into account the uncertainty associated with the estimations, we adopt a simple risk-averse scoring framework that selects k results and maximizes:

$$\max \sum_{i=1}^k \left(|\hat{r}_{Q \bowtie C_i}| * (1 - risk(Q, C_i)) \right) \quad (5)$$

where $|\hat{r}_{Q \bowtie C_i}|$ is the absolute value of the correlation estimate computed using a correlation estimator applied to $L_{Q \bowtie C_i}$, and $risk(Q, C_i)$ is a function that returns a number in the range $[0, 1]$ and measures the dispersion of the correlation estimates using $L_{Q \bowtie C_i}$, such as standard error or confidence interval length. Intuitively, whenever the risk associated with the estimation is non-zero, a penalty factor proportional to the risk is applied to the estimate. Note that we consider the absolute of the correlation in Eq. 5, given that negative correlations can be as useful as positive correlations.

4.2 Measuring the Estimation Error Risk

A natural approach to measure the risk of estimation error is to use standard statistics such as the standard error of the estimator or the length of the confidence interval. In our scenario, however, we do not have access to these: since we do not explicitly join the columns (given that doing so is computationally prohibitive), we have little information about the distributions of column values. For instance, it is not possible to compute the exact variance (and similarly standard deviation or standard error) for the correlation because it depends on the underlying correlation of the complete data and fourth-order moments of the variables [79] (see Equation 4 for the variance under normal distribution assumptions or see [16] for the general case). Moreover, estimating high-order moments using small sample sizes may be unstable [13].

One statistic that we can compute is the standard error of the sampling distribution of the Fisher’s Z correlation transformation [7], given by $SE_z = 1/\sqrt{n-3}$. While it assumes a bivariate normal distribution, its computation is simple and only depends on the known sample size n . Despite the normality assumption, this statistic is asymptotically equivalent to the error found in our theoretical analysis of $1/\sqrt{n}$ (Section 4.3). Thus, we expect it to work increasingly well as the sample size increases for any data distribution.

While we expect the Fisher’s Z standard error to be accurate for large sample sizes, one drawback is that it assumes normality and does not take into account any information about the data distribution. Given that real-world data is seldom normally distributed [55] and the actual data distributions are usually unknown, we are interested in calculating distribution-independent confidence interval bounds. In this setting, non-parametric approaches such as bootstrapping are applicable. Bootstrapping only makes use of the samples generated by our sketches and does not assume any prior data distribution. While bootstrapping has been shown

to have good performance for estimating confidence intervals for non-normal distributions [13], it has the disadvantage of having a very high computational cost – specially in settings like ours where it needs to be computed repeatedly over many columns.

To address the limitations of Fisher’s Z (normality assumption) and bootstrapping-based (high computational cost) methods, in Section 4.3, we derive new confidence bounds using finite-sample concentration bounds for sums of independent random variables. These bounds only depend on the maximum and minimum values in $X_{X \rightarrow Y}$ and $Y_{X \rightarrow Y}$. Since $X_{X \rightarrow Y} \subseteq X$ and $Y_{X \rightarrow Y} \subseteq Y$, the values in these columns lie strictly within the range of values in X and Y . Thus, bounds on the range can be computed with a single pass over the columns (i.e., at the same time we construct the Correlation Sketches). Given that these bounds can be computed in constant time, there is essentially no additional computational overhead.

4.3 Confidence Interval Bounds

As discussed in Section 2.2, one challenge in deriving confidence intervals is that Pearson’s correlation is known to be highly sensitive to individual samples. This prevents directly using e.g., a standard McDiarmid’s inequality to bound the accuracy of an estimate for the correlation. Instead, we use individual Hoeffding inequalities to obtain confidence intervals for each individual component of the correlation estimator, and then apply a union bound to combine these results into an overall confidence interval. This is similar to the approach used for constructing confidence intervals for the sample variance for non-Gaussian data in [6].

Analysis. *Correlation Sketches* estimates the Pearson’s correlation between two columns $X_{X \rightarrow Y}$ and $Y_{X \rightarrow Y}$. Let $C_{low} = \min\{x \in X, y \in Y\}$ and $C_{high} = \max\{x \in X, y \in Y\}$ be upper and lower bounds in columns X and Y , and let $C = C_{high} - C_{low}$. Let $A = X_{X \rightarrow Y} - C_{low}$ and $B = Y_{X \rightarrow Y} - C_{low}$. Since a constant shift does not affect Pearson’s correlation, we note that the correlation between $X_{X \rightarrow Y}$ and $Y_{X \rightarrow Y}$ is equal to:

$$\rho = \frac{\langle A - \mu_A \mathbf{1}, B - \mu_B \mathbf{1} \rangle}{\|A - \mu_A \mathbf{1}\|_2 \|B - \mu_B \mathbf{1}\|_2},$$

where $\mu_A = \frac{1}{N} \sum_{i=1}^N A_i$ and $\mu_B = \frac{1}{N} \sum_{i=1}^N B_i$ are the means of A and B and $\mathbf{1}$ is the all ones vector. This expression is equal to

$$\rho = \frac{v_{A,B} - \mu_A \mu_B}{\sqrt{v_A - \mu_A^2} \sqrt{v_B - \mu_B^2}},$$

where $v_A = \frac{1}{N} \sum_{i=1}^N A_i^2$, $v_B = \frac{1}{N} \sum_{i=1}^N B_i^2$ and $v_{A,B} = \frac{1}{N} \langle A, B \rangle = \frac{1}{N} \sum_{i=1}^N A_i B_i$. Let $a, b \in \mathbb{R}^n$ be vectors containing n samples drawn uniformly without replacement from A, B . According to Theorem 1, the estimate to Pearson’s correlation obtained via our sketches is equivalent to:

$$r = \frac{v_{a,b} - \mu_a \mu_b}{\sqrt{v_a - \mu_a^2} \sqrt{v_b - \mu_b^2}},$$

where $\mu_a = \frac{1}{n} \sum_{i=1}^n a_i$, $\mu_b = \frac{1}{n} \sum_{i=1}^n b_i$, $v_a = \frac{1}{n} \sum_{i=1}^n a_i^2$, $v_b = \frac{1}{n} \sum_{i=1}^n b_i^2$, and $v_{a,b} = \frac{1}{n} \sum_{i=1}^n a_i b_i$.

Union Bound. We want to compute a confidence interval for ρ , meaning that, for some specified α (e.g., $\alpha = .05$), our goal is to compute upper and lower bounds ρ^{low}, ρ^{high} depending on our estimate r such that: $\Pr[\rho^{low} \leq \rho \leq \rho^{high}] \geq (1 - \alpha)$. To do so, we first compute the upper and lower bounds for $\mu_A, \mu_B, v_A, v_B, v_{A,B}$, for all of the 5 parameters r depends on. For any parameter

c , we want: $\Pr[c^{low} \leq c \leq c^{high}] \geq (1 - \alpha/5)$. For example, that $\Pr[\mu_A^{low} \leq \mu_A \leq \mu_A^{high}] \geq (1 - \alpha/5)$. We will discuss how to obtain these bounds shortly, but for now we show how they can be used to compute a confidence interval. First let:

$$\begin{aligned} num_{low} &= v_{A,B}^{low} - \mu_A^{high} \mu_B^{high} & num_{high} &= v_{A,B}^{high} - \mu_A^{low} \mu_B^{low} \\ den_{low} &= \sqrt{\max[0, v_A^{low} - (\mu_A^{high})^2] \cdot \max[0, v_B^{low} - (\mu_B^{high})^2]} \\ den_{high} &= \sqrt{\max[0, v_A^{high} - (\mu_A^{low})^2] \cdot \max[0, v_B^{high} - (\mu_B^{low})^2]} \end{aligned}$$

Then set:

$$\rho^{low} = \begin{cases} \frac{num_{low}}{den_{high}} & \text{if } num_{low} \geq 0 \\ \frac{num_{low}}{den_{low}} & \text{if } num_{low} < 0 \end{cases} \quad (6)$$

$$\rho^{high} = \begin{cases} \frac{num_{high}}{den_{low}} & \text{if } num_{high} \geq 0 \\ \frac{num_{high}}{den_{high}} & \text{if } num_{high} < 0. \end{cases} \quad (7)$$

By a union bound, we have $\Pr[\rho^{low} \leq \rho \leq \rho^{high}] \geq (1 - \alpha)$.

Individual Parameter Bounds. The next step is to obtain the confidence intervals for each of the parameters $\{\mu_A, \mu_B, v_A, v_B, v_{A,B}\}$, which we do using Hoeffding’s concentration inequality for bounded random variables. This bound is usually stated for sampling *with* replacement (i.e., independent random sampling), but Hoeffding proves in his original paper that it also holds for *without* replacement sampling, which only gives better concentration. Specifically Theorems 2 and 4 in [43] give:

Lemma 1 (Hoeffding’s Inequality). *Let X_1, \dots, X_N be a set numbers bounded $\in [0, C]$ with mean $\mu_X = \frac{1}{N} \sum_{i=1}^N X_i$. Let Y_1, \dots, Y_n be drawn independently without replacement from this set. Then:*

$$\Pr \left[\left| \mu_X - \frac{1}{n} \sum_{i=1}^n Y_i \right| \geq t \right] \leq 2e^{-2nt^2/C^2}.$$

Since A and B have values in $[0, C]$ by definition, each of the terms $\{\mu_A, \mu_B, v_A, v_B, v_{A,B}\}$ is the average of N numbers, bounded between $[0, C]$ for μ_A, μ_B and between $[0, C^2]$ for the others. Accordingly, we can apply Hoeffding’s inequality to obtain a confidence interval with $\alpha/5$, as required by our analysis above. For example, consider μ_A . We have from Hoeffding’s that:

$$\Pr[|\mu_A - \mu_a| \geq t] \leq 2e^{-2nt^2/C^2}.$$

For $2e^{-2nt^2/C^2} = \alpha/5$, we solve for $t = \sqrt{\ln(10/\alpha) \cdot C^2/2n}$ and can then set $\mu_A^{low} = \mu_a - t$ and $\mu_A^{high} = \mu_a + t$. As another example, consider v_A . From Hoeffding’s,

$$\Pr[|v_A - v_a| \geq t] \leq 2e^{-2nt^2/C^4}.$$

For $2e^{-2nt^2/C^4} = \alpha/5$, we solve for $t' = \sqrt{\ln(10/\alpha) \cdot C^4/2n}$ and can then set $v_A^{low} = v_a - t'$ and $v_A^{high} = v_a + t'$. Final bounds for all five parameters are as follows:

$$[\mu_A^{low}, \mu_A^{high}] = [\mu_a - t, \mu_a + t], \quad [\mu_B^{low}, \mu_B^{high}] = [\mu_b - t, \mu_b + t]$$

$$[v_A^{low}, v_A^{high}] = [v_a - t', v_a + t'], \quad [v_B^{low}, v_B^{high}] = [v_b - t', v_b + t']$$

$$[v_{A,B}^{low}, v_{A,B}^{high}] = [v_{a,b} - t', v_{a,b} + t']$$

where $t = \sqrt{\ln(10/\alpha) \cdot C^2/2n}$ and $t' = \sqrt{\ln(10/\alpha) \cdot C^4/2n}$.

Discussion. The above analysis gives a simple procedure to compute valid confidence interval for correlation estimates: we first compute t, t' as defined above, which only requires the desired confidence level α , C which is pre-computed, and the sample size n (i.e., the number of rows in $L_{\langle X \triangleright \langle Y \rangle}$). Then, we compute upper and lower bounds for each parameter, and plug into Equations (6) and (7) to obtain a final confidence interval.

Our analysis shows that, for a fixed $1 - \alpha$ confidence level, the confidence interval bounds depend on the sample size and up to the fourth-power of the range C of the variables A and B . This is in line with previous findings which point that the deviation of the Pearson's sample estimator depends on the fourth-moment of the variables [79, 80]. The accuracy of the bound also scales inversely with the square root of the sample size n , as expected.

Correlation is difficult to estimate whenever the population variance is low, because the estimator can become unstable (as these terms appear in the denominator of the equation for r). In particular, if either $\|A - \mu_A \bar{1}\|_2$ or $\|B - \mu_B \bar{1}\|_2$ is close to zero, then any small deviation of $\|a - \mu_a \bar{1}\|_2$ or $\|b - \mu_b \bar{1}\|_2$ from the true values that we are trying to estimate would lead to a large difference in ρ vs. r .

So, to get a better sense of the bounds, let us assume that, for both A and B , $\text{var}(A) = v_A - \mu_A^2$ and $\text{var}(B) = v_B - \mu_B^2$ are $\geq c$ for some constant c . From the analysis above, it is relatively easy to show that if we set $n = O\left(\frac{C^4 \ln(1/\alpha)}{\epsilon^2 c^2}\right)$, we will obtain a final confidence interval with width 2ϵ - i.e., we can estimate the Pearson's correlation to accuracy $\pm\epsilon$. For data bounded by C , it would be natural for the variance c to be on the order of C^2 , in which case, the number of samples required is just $n = O\left(\frac{\ln(1/\alpha)}{\epsilon^2}\right)$. In other words, as the sample size n grows (i.e., as our sketches size increases) our estimate converges with error roughly $\frac{1}{\sqrt{n}}$.

Effect of Small Sample Sizes. Note that when sample sizes are small, the bounds for the standard deviation terms ($v - \mu^2$) may become negative, which makes den_{high} and den_{low} to become zero and thus yield invalid bounds. To address this problem, while computing ρ^{low} and ρ^{high} , we can replace the denominator of the Equations 6 and 7 by the product of the sample standard deviation of the variables computed using the samples induced by the sketch join, i.e., we can set $den_{high} = den_{low} = \sqrt{v_a - \mu_a^2} \sqrt{v_b - \mu_b^2}$. We refer to these modified upper bound and lower bound, respectively, as ρ_{HFD}^{high} and ρ_{HFD}^{low} . Although these are not true probabilistic bounds, their resulting confidence interval length ($\rho_{HFD}^{high} - \rho_{HFD}^{low}$) still provides meaningful information to measure the estimation error risk. This is because the denominator term serves as a normalization factor of the covariance term in the numerator (for which we still compute the true bounds).

4.4 Scoring Functions

Based on the framework (Section 4.1) and statistics (Sections 4.2 and 4.3) described above, we finally derive four different scoring functions that optimize ranking for correlated column discovery.

Let $ci_{length} = \rho_{HFD}^{high} - \rho_{HFD}^{low}$ be the confidence interval length of a correlation estimate. Then, set ci_{max}^{high} and ci_{min}^{high} to be the maximum and the minimum confidence interval length in a ranked list, respectively. We define the following risk penalization factors:

$$se_z = 1 - \frac{1}{\sqrt{\max(4, n) - 3}} \quad ci_b = 1 - \frac{\rho_{PM1}^{high} - \rho_{PM1}^{low}}{2}$$

$$ci_h = 1 - \frac{ci_{length} - ci_{min}^{high}}{ci_{max}^{high} - ci_{min}^{high}}$$

Recall from our framework that each of these factors assume values in the range $[0, 1]$ and when they are equal to 1, the error risk is the minimum possible. The equations above are direct applications of the statistics introduced in Sections 4.2-4.3, i.e., Fisher's Z transformation standard error, Bootstrap CI, and our Hoeffding's CI. By plugging them into Equation 5, we have (in addition, we also consider a no-penalization factor in s_1):

$$s_1 = r_p, \quad s_2 = r_p * se_z,$$

$$s_3 = r_b * ci_b, \quad s_4 = r_p * ci_h,$$

where r_p and r_b are the absolute of the correlation estimated using, respectively, the Pearson's sample estimator and the PM1 bootstrap estimator [72]. We also use PM1 for the confidence intervals in ci_b .

5 EXPERIMENTAL EVALUATION

We performed extensive experiments using both synthetic and real-world datasets to evaluate the effectiveness of *Correlation Sketches* and the proposed ranking strategies.

5.1 Datasets

We used three different data collections: *Synthetic Bivariate Normal*, which is synthetically generated and follows a pre-defined, well-known data distribution; the *World Bank's Finance* [75] and the *NYC Open Data* [58] collections, which contain real-world datasets, currently published in open data portals. We used snapshots of these repositories collected in September 2019 using Socrata's REST API [66]. All datasets were stored in plain CSV text files, and we used the *Tablesaw* library [68] to automatically parse and detect the basic data types for each column.

World Bank Finances (WBF). This collection contains 64 datasets (tables) related to the World Bank's Finances [75]. There is missing data in several columns and some columns contain large monetary values. From each table, we extracted all possible pairs of categorical and numerical data columns ($\langle K_X, X \rangle$), out of which we generated all possible unique 2-combinations of columns pairs - 9,979,278 pairs of column pairs, i.e., $\langle K_X, X \rangle, \langle K_Y, Y \rangle$.

NYC Open Data (NYC). The tables from this dataset contain data published by New York City agencies and their partners [58]. Our snapshot includes 1,505 different datasets. Using the same process described above for the World Bank Finances collection, we generated 12,497,500 pairs of column key-value pairs.

Synthetic Bivariate Normal (SBN). This dataset was generated by creating t tables consisting of n tuples $\langle k, x_k, y_k \rangle$, where $k \in K$ is a random unique string, and $x_k \in X$ and $y_k \in Y$ are real numbers drawn from a bivariate normal distribution with mean $\mu = 0$. The covariance of the column vectors X and Y was chosen in such a way that the Pearson's correlation coefficient between X and Y was approximately equal to a given parameter r_{XY} . We then created t pairs of tables $\mathcal{T}_X = \langle K_X, X \rangle$ and $\mathcal{T}_Y = \langle K_Y, Y \rangle$. Finally, we reduced the size of the table \mathcal{T}_Y from n to n' by selecting a uniform random sample of size $n' = n * c$, where c is a random real number in the

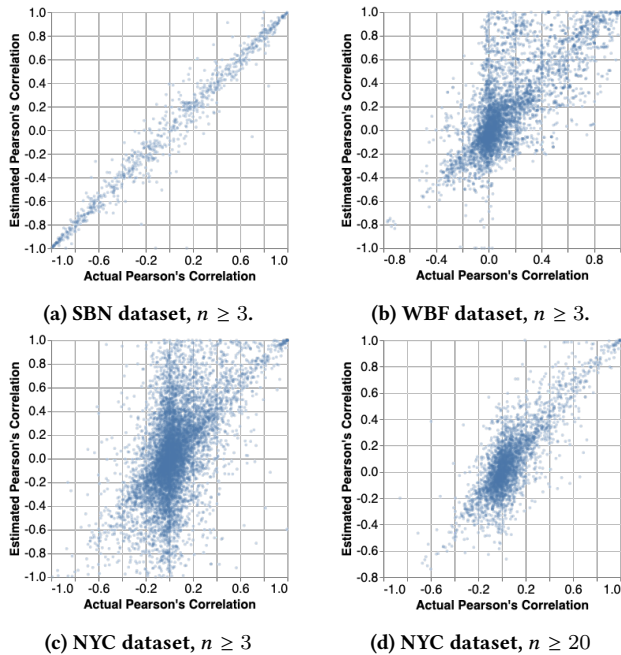


Figure 3: Estimation errors significantly vary for different samples sizes and different datasets with different data distributions. (a), (b), and (c) show the deviations of all column pairs for 3 different datasets. (d) shows the estimates from (c) after filtering out estimates that use fewer than 20 samples.

range $(0, 1)$ indicating the join probability between X and Y . We set the number of table pairs $t = 3000$. For each table pair, we set n to be a random number drawn uniformly in the range $(0, 500000)$, and the correlation r_{XY} is drawn uniformly at random from $(-1, 1)$.

5.2 Correlation Estimation Accuracy

To study the effectiveness of our sketching method, we compare the estimated correlations against the actual correlations. For each pair of columns, $\langle K_X, X \rangle$ and $\langle K_Y, Y \rangle$, we first build their correlation sketches $L_{\langle K_X, X \rangle}$ and $L_{\langle K_Y, Y \rangle}$, and then compute their correlation estimates $\hat{r}_{\langle X \bowtie Y \rangle}$. Then, we compare the estimates with the actual column correlations $r_{X \bowtie Y}$ computed using the (complete) join of columns $X_{X \bowtie Y}$ and $Y_{X \bowtie Y}$. Due to space limitations, we show the results for Pearson’s correlation. We discuss the performance of other estimators in Section 5.3.

Figure 3 shows scatterplots for the estimates computed for all three datasets against the actual Pearson’s correlation values, using sketches of size 256. We can clearly see that *Correlation Sketches* produces quite accurate results for the SBN dataset (Figure 3a), which contains only data drawn from a bivariate normal distribution: the estimates are concentrated close to their actual correlation values with only a few points deviating from the actual correlation values.

For the NYC (Figure 3b) and WBF (Figure 3c) datasets, which contain real-world data from unknown distributions, as expected, there are more incorrect predictions. We can observe that for many points with actual correlation equal to 0, the correlation is overestimated – see the vertical line around the value zero in the x-axis. This happens because some of the joins computed from the sketches

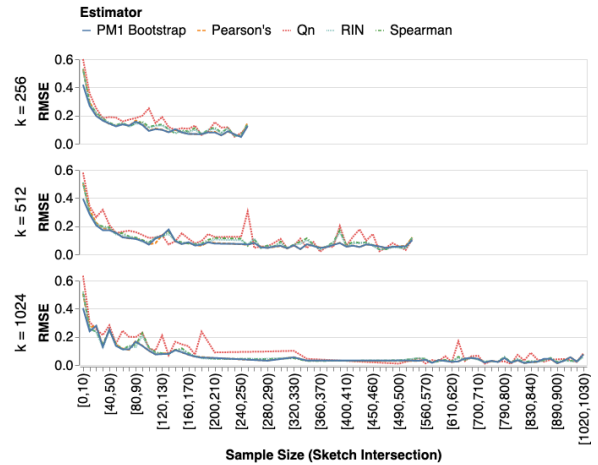


Figure 4: The sample size (sketch intersection) has an impact on RMSE. As the sketch intersection size increases, the RMSE decreases in the NYC dataset. Here, the k parameter (row) denotes the maximum sketch size (number of minimum values kept in the sketch).

can be too small, leading to this inaccuracy. Note that Figures 3a, b, and c reflect estimates computed with joins (sketch intersection) that contain as few as 3 tuples ($n \geq 3$). Nonetheless, we can still observe a large concentration of points around the diagonal line, suggesting that *Correlation Sketches* is effective.

To better understand the behavior of the sketches with respect to sample size, we also plot in Figure 3d the results for the NYC data showing only join samples with size at least 20. The plot shows that indeed, for larger sample sizes, the behavior is more similar to that of the SBN dataset – the points are more concentrated closer to the diagonal, indicating the estimates are more accurate.

This provides evidence for the issue we discussed in Section 4: in large table collections, there are often many more poorly-correlated tables than well-correlated ones, and estimation errors may lead to a potentially large number of false positives. This underscores the importance of having effective ranking functions to help users focus their attention on tables that are more likely to be correlated. In this case, for example, a ranking function that prioritizes estimates computed from larger join samples is likely to be effective at pruning these false positive results.

5.3 Exploring Different Correlation Estimators

We studied the performance of different correlation estimators:

(1) *Pearson’s Sample Correlation*: Computes the correlation using the formula defined in Equation 3.

(2) *Spearman’s Rank Correlation*: Let $r(x) = r_x$ where $r_x = 1$ for the smallest x , $r_x = 2$ for the second smallest x , and so on. The numeric column values are transformed using $r(x)$ and then the Pearson’s correlation over the transformed values is computed.

(3) *Rank-based Inverse Normal (RIN)*: Similarly to Spearman’s, a transformation function is applied before computing the Pearson’s correlation. Following [11], we employ the *rankit* function [14] which is defined as: $h(x) = \Phi^{-1} \left(\frac{r(x)-1/2}{n} \right)$, where Φ is the inverse normal cumulative distribution function.

ranker	score	%	ranker	score	%	ranker	score	%	ranker	score	%
$r_p * ci_h$	0.529	193.2%	$r_p * se_z$	0.472	102.1%	$r_b * ci_b$	0.714	51.5%	$r_b * ci_b$	0.845	17.7%
$r_b * ci_b$	0.516	185.9%	$r_p * ci_h$	0.467	99.8%	$r_p * ci_h$	0.705	49.5%	r_p	0.843	17.5%
r_p	0.507	180.9%	r_p	0.452	93.2%	r_p	0.699	48.4%	$r_p * ci_h$	0.841	17.3%
$r_p * se_z$	0.420	133.1%	$r_b * ci_b$	0.428	83.2%	$r_p * se_z$	0.689	46.2%	$r_p * se_z$	0.832	15.9%
jc	0.180	0.0%	\hat{jc}	0.239	2.3%	random	0.481	2.1%	jc	0.726	1.2%
\hat{jc}	0.172	-4.8%	jc	0.234	0.0%	\hat{jc}	0.480	1.8%	random	0.724	0.9%
random	0.161	-10.8%	random	0.202	-13.7%	jc	0.471	0.0%	jc	0.717	0.0%

(a) MAP ($r > .75$) (b) MAP ($r > .50$) (c) nDCG@5 (d) nDCG@10

Table 1: Ranking evaluation scores in terms of MAP and nDCG. The “%” column denotes relative improvement over jc .

(4) Q_n correlation: Computes the correlation using as modified formula of Pearson’s correlation and the robust Q_n scale estimator. For more details, see [64].

(5) $PM1$ Bootstrap: Performs repeated re-sampling with replacement of the data and recomputes the correlation using the Pearson’s sample correlation estimator. The average of all re-samples is then used as an estimate. Instead of drawing a fixed large number of re-samples (say 10,000), we stop the re-sampling when the probability of changing the mean by more than 0.01 falls below 0.05%.

Most computed correlation estimates using sketches were compared to their corresponding population correlations (i.e., including the transformations of the population data when applicable). The only exception was the $PM1$ Bootstrap estimator, which is compared to the population’s Pearson’s correlation that it intends to estimate.

Correlation estimators differ in their sample size requirements and sensitivity to the data distribution [15]. To better understand how the correlation estimation accuracy changes when we vary the estimator and the amount of storage space used by the sketch (determined by the maximum sketch size), we plot the root mean squared error (RMSE) for different choices of correlation estimators and maximum sketch sizes in Figure 4. We can see a trend: for all estimators and maximum sketch sizes, the RMSE decreases as the intersection size between the sketches increases. The RMSE stabilizes roughly at 0.1. While the different estimators display similar trends, the plot also shows that some estimators are less robust (see e.g., the spikes in the line for Q_n).

5.4 Correlated Column Ranking

To better understand the effectiveness of the proposed scoring functions, we use the NYC data collection which contains the largest number of tables. For each pair of columns $\langle K_X, X \rangle$ in the collection, we retrieved all other joinable columns $\langle K_Y, Y \rangle$. Then, we ranked the list of retrieved columns using the scoring functions described in Section 4. As baselines we use: 1) a *random* scoring function, which assigns random scores in the range $[0, 1]$ drawn from a uniform distribution; 2) the *exact* Jaccard Containment (jc) similarity computed using the complete data after the join; and 3) the JC similarity estimated (\hat{jc}) using our correlation sketches. Even though these baselines do not take correlation into account, we use them as a point of comparison, since they represent existing methods for retrieving joinable tables.

We use two well-known measures to compare the scoring functions: mean average precision (MAP) and normalized discounted cumulative gain (nDCG) [47]. nDCG supports graded relevance judgments, i.e., each retrieved column can receive different scores

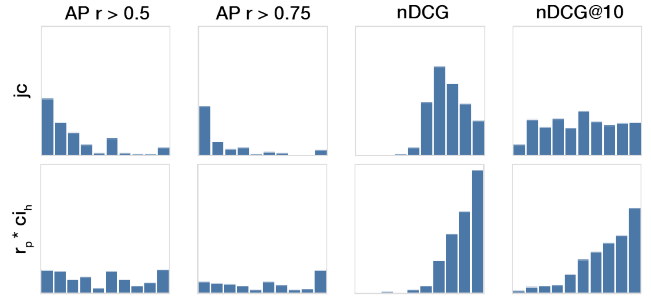


Figure 5: Distribution of the evaluation metric scores for different scoring functions. x -axis shows slices of the metric range $[0, 1]$. Each bar corresponds to a slice of width 0.1. The y -axis show the number of queries that fall in each slice.

depending on their relevance (the absolute value of the correlation, in our case) and position on the list. In contrast, MAP supports binary judgment, and relies on thresholds to decide which columns are relevant (say, $r > .5$).

To evaluate different aspects of the ranking, we compute MAP for the whole ranked list using different thresholds for correlation relevance: $r > 0.50$ and $r > 0.75$. For nDCG, which has a tendency of assigning higher scores, we compute the metrics only over the top- k search results, where $k = 5$ and $k = 10$. Table 1 summarizes the results. The first trend we observe is that the ranking produced using the JC similarity scores attains scores similar to random ordering. This confirms our hypothesis that JC is not well suited for ranking the results of join-correlation queries and also suggests that highly-correlated columns can have different levels of JC similarity.

Note that all correlation-based ranking functions (Section 4.4) show significant improvements over the baselines. The ranking functions based on our Hoeffding bounds ($r_p * ci_h$) attain scores that are either better or very close to the bootstrap-based ranking function. This is specially interesting due to the fact that the Hoeffding-based CI can be computed in constant time, in contrast to the bootstrap method that requires many re-samples and the computation of correlations for these samples (typically, around between 1,000 and 10,000 iterations are used [12, 13]). In other words, we derive rankings that are comparable to those produced by the bootstrapping at a fraction of the cost. Moreover, the MAP scores suggest that the Hoeffding-based scoring is particularly effective at avoiding false positives with correlation above $r > 0.75$.

Table 1 shows only average scores over all queries. To get a better sense for the improvements over all queries, we plot the

distribution of evaluation scores in Figure 5. The histograms show the number of queries for different metric score values. Rows display the scoring functions: JC similarity (first row) and the Hoeffding-based scoring (second row). We can clearly see that, for all metrics, the scores distributions shift from left (bad scores) to right (good scores), indicating improvements in the whole metric range. It is also clear that, specially when considering the nDCG metric, most queries have very good scores (i.e., close to the optimal).

5.5 Running Time

Join-Correlation Estimation. To assess the efficiency of our approach and suitability for use in dataset search engines, we compare the running times of joins and correlation estimation computations using the sketches against the times required to execute the same computation over the full data. Since *Correlation Sketches* creates fixed-sized synopses for arbitrarily-sized datasets, it is natural to expect a big performance impact due to the reduction in the complexity of the problem – from potentially large table sizes to a small constant factor (sketch size). The results are summarized in Table 2. Due to space limitations we only include the times for joins and correlation computations using Pearson’s and Spearman’s coefficients. The results confirm that, with sketches, queries can be evaluated orders of magnitude faster than by using the full data, and given that the sketch size is fixed, their running time is more predictable. Note that, for this comparison, we assume the data is loaded in memory. However, for large datasets, the costs associated with using the full data would be even higher due to the cost of reading data from disk or transferring it over a network.

Query Evaluation. We also assessed the performance of evaluating join-correlation queries. For this experiment, we extracted all column pairs $\langle K_X, X \rangle$ from all 1,505 tables in the NYC dataset and randomly split them into two distinct sets, which we denote as *query set* and *corpus set*. Next, we set the maximum sketch size to 1024 and built an inverted index for all tables of the corpus set using a standard indexing library [2]. Finally, we used all pairs from the *query set* to issue queries against the index and measured the query execution time. We observed that the running times for 94% of queries are under 100 ms and $\sim 98.5\%$ of queries take under 200 ms. These times include retrieving the top-100 columns by key overlap, reading sketches from the index, and re-sorting all columns by estimated correlation. These preliminary results are promising and suggest that our approach can provide interactive response times for join-correlation queries over large data collections.

6 RELATED WORK

Our work builds on a large body of research that includes sampling and sketching algorithms used to handle massive data streams [26], join size estimation [42], and the statistics literature on correlations. Also related to our work is recent research on dataset search [17, 81], and methods that support data augmentation queries which, given a query dataset, find datasets that can be joined or concatenated [20, 56, 77, 84, 85] or that contain related entities [52, 82].

Cardinality Estimation. Several methods have been proposed that summarize massive datasets into succinct data structures to

percentiles	Full data			Sketch		
	join	r_s	r_p	join	r_p	r_s
mean	42.219	8.494	0.240	0.026	0.000	0.004
std. dev.	367.696	134.357	9.314	5.618	0.042	0.279
75%	0.231	0.141	0.005	0.003	0.000	0.002
90%	7.038	0.154	0.011	0.006	0.001	0.004
99%	1360.605	29.583	0.385	0.012	0.003	0.013
99.9%	4021.838	2731.154	51.278	0.021	0.007	0.033

Table 2: Running times (in milliseconds) for computing joins and correlations using full data and sketches. Using the full data, queries can take orders of magnitude more time than when using the sketches. r_s denotes the Spearman’s estimator and r_p denotes Pearson’s estimator.

support approximate queries using bounded memory [26]. A widely-studied problem in this area is cardinality estimation, i.e., estimating the number of distinct elements in a set. Approaches to this problem can be broadly classified into two groups: sampling and sketch-based algorithms. *Sampling algorithms* avoid scanning the full dataset and estimate cardinalities based on data samples. These algorithms have been criticized for their inability to provide a good error guarantees [21, 41]. In contrast, *sketch-based algorithms* fully scan the dataset once, compute hashes of the items, and create a sketch that can be used to compute cardinality estimates [5, 8, 9, 24, 25, 29, 33, 69]. Harmouch and Naumann [42] categorized algorithms these into different families: *count trailing 1s*, *count leading 0s*, *k^{th} minimum values*, and *linear synopses*. Each of these families has their best algorithms which exhibit different trade-offs, which were studied in detail in [42].

While the best algorithms based on counting trailing 1s and 0s (such as HyperLogLog (HLL) [37]) are able to provide better accuracy per bit, it is not clear how they can be extended to estimate cardinalities of value-sets that satisfy arbitrary properties not known apriori, before the sketch is built. Algorithms from the *k^{th} minimum values (KMV) family*, on the other hand, can be extended for this purpose at the cost of storing the sample identifiers in addition to their hashed values [28]. The reason why HLL-like algorithms cannot estimate such properties is that, HLL does not maintain any sample of identifiers from the data. For this same reason, HLL sketches are not suitable for join-correlation sketches, which require alignment of numeric values based on their join key values. *Correlation Sketches* builds on the KMV family and derives a new sketch that is able to align numeric values based on their key hashed values to reconstruct a random samples that can ultimately be used for estimating correlations. While we focus on correlations in this paper, the sketches we propose can be used to compute any statistics that are based on paired numeric values (e.g., distance correlations [67] and the entropy-based mutual information).

Join Size Estimation. The ability to accurately estimate join sizes is crucial for query optimizers. Acharya et al. [1] have established very early results on the hardness of sampling over joins, in the general foreign-key setting, by showing that it is generally not possible to create a uniform random sample by simply joining uniform random samples from each independent relation. Since then, approaches have been developed to address this problem, which can be broadly grouped in the following categories: sampling, sketching, indexing, and machine learning.

Sketching-based algorithms [63] leverage the techniques mentioned above to create sketches on the join attribute and ignoring all the other attributes. These algorithms usually provide accurate estimates on the join size on queries without selection predicates. In order to support queries with predicates, however, 2-way joins need to be transformed into 3-way joins by creating an additional sketch to represent the predicate [22], which substantially deteriorates the estimation quality [71].

Sampling-based algorithms keep a sample of the tuples, apply predicates on the sample to select the tuples that satisfy them, and finally estimate the join size using only these tuples. Multiple tuple-sampling strategies have been proposed [1, 22, 35, 71]. Recent works [22, 71] incorporate ideas similar to the strategy used in this paper and in KMV sketches family: they use a random hashing function to map join values to the unit range and then select tuples based on some selection strategy. For instance, the strategy adopted by the correlated sampling algorithm [71] is equivalent to the strategy of the G-KMV sketch [77], where tuples are selected if the hashed keys are smaller than a probability threshold. In contrast, *Correlation Sketches* includes tuples in the sketch up to a fixed number, which avoids assigning too much space to large datasets and leads to more predictable performance for query evaluation. In the future, we would like to explore trade-offs between the fixed-sized sketches we use and variable-sized sketches.

Index-assisted algorithms [38, 53, 54] rely on indexes to perform the sampling. The use of indexes allows algorithms to retrieve only tuples that are relevant to the query, thus avoiding worst-case scenarios where no samples are available to perform estimations. A drawback of this approach is that indexes are not always available, and repeated index look-ups become expensive when the index does not fit into main memory.

When a join involves keys of multiple tables and highly-selective predicates, it becomes harder to estimate the join size because the join keys intersection gets increasingly smaller. Recently proposed approaches based on *machine-learning* [48, 78] are able to improve the estimation performance for highly-selective worst-case queries.

There are key differences between our work and approaches to join-size estimation algorithms both in terms of their goals and challenges. Notably, *Correlation Sketches* does not need to deal with selection conditions, and one-many as well as many-many relationships can be reduced to one-one joins (Section 3), allowing us to create uniform random samples of the resulting join table.

Dataset Discovery and Search. Given an input query dataset, dataset discovery methods have been proposed to find related datasets that can be integrated via relational operations *join* or *union*. They use the notions of Jaccard similarity and containment, along with variations, to compute overlaps in dataset keys and other categorical attributes. These overlaps are then used to estimate how *joinable* or *unionable* two datasets are. JOSIE [84] provides an exact solution for finding joinable datasets in a data lake. LSH Ensemble [85], GB-KMV [77] and Lazo [20] propose approximate approaches to the same problem. Nargesian et al. [56] proposed a probabilistic solution to the problem of searching for unionable tables within massive data repositories. While these works focus on either finding datasets that are joinable or union-able, we focus on finding joinable tables that have highly correlated columns.

Several end-to-end dataset search systems have also been proposed. Data Civilizer [31] is a system that uses a linkage graph to help identification of relevant data to a user task. JUNEAU [83] formalized multiple data search tasks, table relatedness measures (e.g., column and row overlap, provenance, textual similarity), and proposed a linear combinations of these measures for providing data search within data science environments. ARDA [23] is a system that focuses on automatic data augmentation, i.e., how select the best features discovered from external dataset search systems. We address an orthogonal problem: instead of building an end-to-end system, we focus on *efficient* discovery and computation of a class of relationships that has been overlooked in prior works: correlation between numeric variables. Our techniques can be integrated as relationships in linkage graphs [31, 36] or as a table relatedness measure [83] to improve search applications.

Correlation Estimation. Correlation measures have been studied extensively in the literature (Section 2.2). Most works in this area focus on statistical inference, i.e., given samples of a potentially infinite population, the goal is to infer properties by deriving estimates or performing statistical tests. Recent work has focused on reducing bias and estimation errors [11], hypothesis testing [10, 30], or confidence intervals (CI) that work well under non-normal distributions [12, 13, 44]. Differently from existing CIs, we develop a CI for sub-samples based on concentration inequalities that makes no distributional assumptions. This setting is particularly attractive for sketching algorithms that perform a single pass over the data, allowing us to leverage statistics about data (e.g., the range of the values) which would otherwise be unknown.

7 CONCLUSION

In this paper, we studied a new class of data discovery queries, *join-correlation queries*, and proposed a new approach to support them based on data sketches for join-correlation estimation. We also developed confidence interval bounds for the accuracy of these correlation estimates, and used them to design functions to rank the discovered columns. We experimentally evaluated both our sketches and scoring functions and showed that they are effective in a variety of datasets and different correlation measures.

While we focused on correlations, our sketches are general and may be used to estimate other statistics. Moreover, our work opens up a new avenue for the development of a new family of sketches that both join and estimate different data relationships between unjoined datasets. For future work, we plan to explore different approaches to derive tighter confidence bounds, compare the performance and effectiveness sample selection strategies [28, 77], and investigate a tighter integration between our method and others that focus on finding joinable datasets (e.g., Lazo [36] and JOSIE [84]). Finally, we would like to explore applications of our sketches for building end-to-end data search that takes into account the improvement in accuracy of machine learning models.

Acknowledgments. This work was partially supported by the DARPA D3M program and NSF award OAC-1640864. Any opinions, findings, and conclusions or recommendations expressed in this material are those of the authors and do not necessarily reflect the views of NSF and DARPA.

REFERENCES

- [1] S. Acharya, P. B. Gibbons, V. Poosala, and S. Ramaswamy. Join synopses for approximate query answering. *SIGMOD Rec.*, 28(2):275–286, June 1999.
- [2] Apache lucene. <https://lucene.apache.org/index.html>.
- [3] M. Baak, R. Koopman, H. Snoek, and S. Klous. A new correlation coefficient between categorical, ordinal and interval variables with pearson characteristics. *Computational Statistics & Data Analysis*, page 107043, 2020.
- [4] S. Bapat. Discover, understand and manage your data with Data Catalog, now GA. <https://cloud.google.com/blog/products/data-analytics/data-catalog-metadata-management-now-generally-available>, 2020. [Online; accessed 22-June-2020].
- [5] Z. Bar-Yossef, T. S. Jayram, R. Kumar, D. Sivakumar, and L. Trevisan. Counting distinct elements in a data stream. In J. D. P. Rolim and S. Vadhan, editors, *Randomization and Approximation Techniques in Computer Science*, pages 1–10, Berlin, Heidelberg, 2002. Springer Berlin Heidelberg.
- [6] R. Bardenet, O.-A. Maillard, et al. Concentration inequalities for sampling without replacement. *Bernoulli*, 21(3):1361–1385, 2015.
- [7] K. J. Berry and P. W. Mielke Jr. A monte carlo investigation of the fisher z transformation for normal and nonnormal distributions. *Psychological Reports*, 87(3_suppl):1101–1114, 2000.
- [8] K. Beyer, R. Gemulla, P. J. Haas, B. Reinwald, and Y. Sismanis. Distinct-value synopses for multiset operations. *Commun. ACM*, 52(10):87–95, Oct. 2009.
- [9] K. Beyer, P. J. Haas, B. Reinwald, Y. Sismanis, and R. Gemulla. On synopses for distinct-value estimation under multiset operations. In *Proceedings of the 2007 ACM SIGMOD International Conference on Management of Data*, SIGMOD '07, pages 199–210, New York, NY, USA, 2007. ACM.
- [10] A. J. Bishara and J. B. Hittner. Testing the significance of a correlation with non-normal data: Comparison of Pearson, Spearman, transformation, and resampling approaches. *Psychological Methods*, 2012.
- [11] A. J. Bishara and J. B. Hittner. Reducing bias and error in the correlation coefficient due to nonnormality. *Educational and Psychological Measurement*, 75(5):785–804, 2015.
- [12] A. J. Bishara and J. B. Hittner. Confidence intervals for correlations when data are not normal. *Behavior Research Methods*, 49(1):294–309, 2017.
- [13] A. J. Bishara, J. Li, and T. Nash. Asymptotic confidence intervals for the pearson correlation via skewness and kurtosis. *British Journal of Mathematical and Statistical Psychology*, 71(1):167–185, 2018.
- [14] C. I. Bliss et al. Statistics in biology. statistical methods for research in the natural sciences. *Statistics in biology. Statistical methods for research in the natural sciences.*, 1967.
- [15] D. Bonett and T. A. Wright. Sample size requirements for estimating pearson, kendall and spearman correlations. *Psychometrika*, 65(1):23–28, 2000.
- [16] A. Bowley. The standard deviation of the correlation coefficient. *Journal of the American Statistical Association*, 23(161):31–34, 1928.
- [17] D. Brickley, M. Burgess, and N. Noy. Google dataset search: Building a search engine for datasets in an open web ecosystem. In *The World Wide Web Conference, WWW '19*, pages 1365–1375, New York, NY, USA, 2019. ACM.
- [18] P. Brown, P. J. Haas, J. Myllymaki, H. Pirahesh, B. Reinwald, and Y. Sismanis. Toward automated large-scale information integration and discovery. In *Data Management in a Connected World*, volume 3551 of *Lecture Notes in Computer Science*, pages 161–180. Springer, 2005.
- [19] M. J. Cafarella, A. Halevy, D. Z. Wang, E. Wu, and Y. Zhang. Webtables: exploring the power of tables on the web. *Proceedings of the VLDB Endowment*, 1(1):538–549, 2008.
- [20] R. Castro Fernandez, J. Min, D. Nava, and S. Madden. Lazo: A cardinality-based method for coupled estimation of jaccard similarity and containment. In *2019 IEEE 35th International Conference on Data Engineering (ICDE)*, pages 1190–1201, April 2019.
- [21] M. Charikar, S. Chaudhuri, R. Motwani, and V. Narasayya. Towards estimation error guarantees for distinct values. In *Proceedings of the Nineteenth ACM SIGMOD-SIGACT-SIGART Symposium on Principles of Database Systems, PODS '00*, page 268–279, New York, NY, USA, 2000. Association for Computing Machinery.
- [22] Y. Chen and K. Yi. Two-level sampling for join size estimation. In *Proceedings of the 2017 ACM International Conference on Management of Data, SIGMOD '17*, page 759–774, New York, NY, USA, 2017. Association for Computing Machinery.
- [23] N. Chepurko, R. Marcus, E. Zraggen, R. C. Fernandez, T. Kraska, and D. Karger. Arda: Automatic relational data augmentation for machine learning. *Proceedings of the VLDB Endowment*, 13(9), 2020.
- [24] E. Cohen and H. Kaplan. Tighter estimation using bottom k sketches. *Proc. VLDB Endow.*, 1(1):213–224, Aug. 2008.
- [25] R. Cohen, L. Katzir, and A. Yehezkel. A minimal variance estimator for the cardinality of big data set intersection. In *Proceedings of the 23rd ACM SIGKDD International Conference on Knowledge Discovery and Data Mining, KDD '17*, page 95–103, New York, NY, USA, 2017. Association for Computing Machinery.
- [26] G. Cormode, M. N. Garofalakis, P. J. Haas, and C. Jermaine. Synopses for massive data: Samples, histograms, wavelets, sketches. *Foundations and Trends in Databases*, 4(1-3):1–294, 2012.
- [27] S. Dahlgaard, M. B. T. Knudsen, and M. Thorup. Practical hash functions for similarity estimation and dimensionality reduction. In *Proceedings of the 31st International Conference on Neural Information Processing Systems, NIPS'17*, page 6618–6628, Red Hook, NY, USA, 2017. Curran Associates Inc.
- [28] A. Dasgupta, K. J. Lang, L. Rhodes, and J. Thaler. A Framework for Estimating Stream Expression Cardinalities. In W. Martens and T. Zeume, editors, *19th International Conference on Database Theory (ICDT 2016)*, volume 48 of *Leibniz International Proceedings in Informatics (LIPIcs)*, pages 6:1–6:17, Dagstuhl, Germany, 2016. Schloss Dagstuhl–Leibniz-Zentrum fuer Informatik.
- [29] A. Dasgupta, K. J. Lang, L. Rhodes, and J. Thaler. A Framework for Estimating Stream Expression Cardinalities. In W. Martens and T. Zeume, editors, *19th International Conference on Database Theory (ICDT 2016)*, volume 48 of *Leibniz International Proceedings in Informatics (LIPIcs)*, pages 6:1–6:17, Dagstuhl, Germany, 2016. Schloss Dagstuhl–Leibniz-Zentrum fuer Informatik.
- [30] J. C. de Winter, S. D. Gosling, and J. Potter. Comparing the pearson and spearman correlation coefficients across distributions and sample sizes: A tutorial using simulations and empirical data. *Psychological Methods*, 2016.
- [31] D. Deng, R. C. Fernandez, Z. Abedjan, S. Wang, M. Stonebraker, A. K. Elmagarmid, I. F. Ilyas, S. Madden, M. Ouzzani, and N. Tang. The data civilizer system. In *Cidr*, 2017.
- [32] S. J. Devlin, R. Gnanadesikan, and J. R. Kettenring. Robust estimation and outlier detection with correlation coefficients. *Biometrika*, 62(3):531–545, 12 1975.
- [33] N. Duffield, C. Lund, and M. Thorup. Priority sampling for estimation of arbitrary subset sums. *J. ACM*, 54(6):32–es, Dec. 2007.
- [34] B. Efron and R. Tibshirani. *An Introduction to the Bootstrap*. Chapman & Hall/CRC Monographs on Statistics & Applied Probability. Taylor & Francis, 1994.
- [35] C. Estan and J. F. Naughton. End-biased samples for join cardinality estimation. In *22nd International Conference on Data Engineering (ICDE'06)*, pages 20–20, 2006.
- [36] R. C. Fernandez, Z. Abedjan, F. Koko, G. Yuan, S. Madden, and M. Stonebraker. Aurum: A Data Discovery System. In *ICDE '18*, pages 1001–1012, 2018.
- [37] P. Flajolet, É. Fusy, O. Gandouet, and F. Meunier. HyperLogLog: the analysis of a near-optimal cardinality estimation algorithm. In P. Jacquet, editor, *AofA: Analysis of Algorithms*, volume DMTCS Proceedings vol. AH, 2007 Conference on Analysis of Algorithms (AofA 07) of *DMTCS Proceedings*, pages 137–156, Juan les Pins, France, June 2007. Discrete Mathematics and Theoretical Computer Science.
- [38] S. Ganguly, P. B. Gibbons, Y. Matias, and A. Silberschatz. Bifocal sampling for skew-resistant join size estimation. *SIGMOD Rec.*, 25(2):271–281, June 1996.
- [39] M. Grover. Amundsen — Lyft's data discovery & metadata engine. <https://eng.lyft.com/amundsen-lyfts-data-discovery-metadata-engine-62d27254fb9>, 2019. [Online; accessed 20-October-2019].
- [40] M. Grover. Data Catalog Market | Size & Growth Report, 2020-2027. <https://www.reportsanddata.com/report-detail/data-catalog-market>, 2020. [Online; accessed 28-March-2021].
- [41] P. J. Haas, J. F. Naughton, S. Seshadri, and L. Stokes. Sampling-based estimation of the number of distinct values of an attribute. In *Proceedings of the 21th International Conference on Very Large Data Bases, VLDB '95*, page 311–322, San Francisco, CA, USA, 1995. Morgan Kaufmann Publishers Inc.
- [42] H. Harmouch and F. Naumann. Cardinality estimation: An experimental survey. *Proc. VLDB Endow.*, 11(4):499–512, Dec. 2017.
- [43] W. Hoeffding. Probability inequalities for sums of bounded random variables. *Journal of the American Statistical Association*, 58(301):13–30, 1963.
- [44] X. Hu, A. Jung, and G. Qin. Interval estimation for the correlation coefficient. *The American Statistician*, 74(1):29–36, 2020.
- [45] D. Huang, D. Y. Yoon, S. Pettie, and B. Mozafari. Joins on samples: A theoretical guide for practitioners. *arXiv preprint arXiv:1912.03443*, 2019.
- [46] Y. E. Ioannidis. The history of histograms (abridged). In *VLDB*, pages 19–30, 2003.
- [47] K. Järvelin and J. Kekäläinen. Cumulated gain-based evaluation of ir techniques. *ACM Transactions on Information Systems (TOIS)*, 20(4):422–446, 2002.
- [48] A. Kipf, T. Kipf, B. Radke, V. Leis, P. A. Boncz, and A. Kemper. Learned cardinalities: Estimating correlated joins with deep learning. In *CIDR 2019, 9th Biennial Conference on Innovative Data Systems Research, Asilomar, CA, USA, January 13-16, 2019, Online Proceedings*. www.cidrdb.org, 2019.
- [49] D. Knuth, Addison-Wesley, and P. Education. *The Art of Computer Programming*. Number v. 3 in Addison-Wesley series in computer science and information processing. Addison-Wesley, 1997.
- [50] M. Lan. DataHub: A generalized metadata search & discovery tool. <https://engineering.linkedin.com/blog/2019/data-hub>, 2019. [Online; accessed 22-June-2020].
- [51] O. Lehmberg, D. Ritze, R. Meusel, and C. Bizer. A large public corpus of web tables containing time and context metadata. In *Proceedings of the 25th International Conference Companion on World Wide Web*, pages 75–76, 2016.
- [52] O. Lehmberg, D. Ritze, P. Ristoski, R. Meusel, H. Paulheim, and C. Bizer. The mannheim search join engine. *Journal of Web Semantics*, 35:159 – 166, 2015.

- [53] V. Leis, B. Radke, A. Gubichev, A. Kemper, and T. Neumann. Cardinality estimation done right: Index-based join sampling. In *CIDR 2017, 8th Biennial Conference on Innovative Data Systems Research, Chaminade, CA, USA, January 8-11, 2017, Online Proceedings*. www.cidrdb.org, 2017.
- [54] R. J. Lipton, J. F. Naughton, and D. A. Schneider. Practical selectivity estimation through adaptive sampling. *SIGMOD Rec.*, 19(2):1–11, May 1990.
- [55] T. Micceri. The unicorn, the normal curve, and other improbable creatures. *Psychological bulletin*, 105(1):156, 1989.
- [56] F. Nargesian, E. Zhu, K. Q. Pu, and R. J. Miller. Table union search on open data. *Proceedings of the VLDB Endowment*, 11(7):813–825, 2018.
- [57] Nyc vision zero initiative. <http://www1.nyc.gov/site/visionzero/index.page>.
- [58] NYC OpenData. <https://opendata.cityofnewyork.us>.
- [59] United States Government Open Data. <https://www.data.gov>.
- [60] S. Padmanabhan, B. Bhattacharjee, T. Malkemus, L. Cranston, and M. Huras. Multi-dimensional clustering: A new data layout scheme in DB2. In *SIGMOD*, pages 637–641, 2003.
- [61] C. R. Rao. *Linear Statistical Inference and Its Applications*. Wiley, New York, 1973.
- [62] J. L. Rodgers and W. A. Nicewander. Thirteen ways to look at the correlation coefficient. *The American Statistician*, 42(1):59–66, 1988.
- [63] F. Rusu and A. Dobra. Sketches for size of join estimation. *ACM Trans. Database Syst.*, 33(3), Sept. 2008.
- [64] G. L. Shevlyakov and H. Oja. *Robust correlation: Theory and applications*, volume 3. John Wiley & Sons, 2016.
- [65] G. Shieh. Estimation of the simple correlation coefficient. *Behavior Research Methods*, 42(4):906–917, 2010.
- [66] The Socrata Open Data API. <https://dev.socrata.com>.
- [67] G. J. Székely, M. L. Rizzo, and N. K. Bakirov. Measuring and testing dependence by correlation of distances. *Ann. Statist.*, 35(6):2769–2794, 12 2007.
- [68] The Tablesaw Library. <https://github.com/jtablesaw/tablesaw>.
- [69] D. Ting. Towards optimal cardinality estimation of unions and intersections with sketches. In *Proceedings of the 22nd ACM SIGKDD International Conference on Knowledge Discovery and Data Mining*, pages 1195–1204, 2016.
- [70] P. Venetis, Y. Sismanis, and B. Reinwald. Crsi: a compact randomized similarity index for set-valued features. In *Proceedings of the 15th International Conference on Extending Database Technology*, pages 384–395, 2012.
- [71] D. Vengerov, A. C. Menck, M. Zait, and S. P. Chakkappen. Join size estimation subject to filter conditions. *Proc. VLDB Endow.*, 8(12):1530–1541, Aug. 2015.
- [72] R. R. Wilcox. Confidence intervals for the slope of a regression line when the error term has nonconstant variance. *Computational Statistics & Data Analysis*, 22(1):89–98, 1996.
- [73] C. C. Williams. Democratizing Data at Airbnb. <https://medium.com/airbnb-engineering/democratizing-data-at-airbnb-852d76c51770>, 2017. [Online; accessed 22-June-2020].
- [74] World Bank Open Data. <https://data.worldbank.org>.
- [75] World Bank Group Finances. <https://finances.worldbank.org>.
- [76] C. Xiao, W. Wang, X. Lin, J. X. Yu, and G. Wang. Efficient similarity joins for near-duplicate detection. *ACM Transactions on Database Systems (TODS)*, 36(3):1–41, 2011.
- [77] Y. Yang, Y. Zhang, W. Zhang, and Z. Huang. Gb-kmv: An augmented kmv sketch for approximate containment similarity search. In *2019 IEEE 35th International Conference on Data Engineering (ICDE)*, pages 458–469, April 2019.
- [78] Z. Yang, E. Liang, A. Kamsetty, C. Wu, Y. Duan, X. Chen, P. Abbeel, J. M. Hellerstein, S. Krishnan, and I. Stoica. Deep unsupervised cardinality estimation. *Proc. VLDB Endow.*, 13(3):279–292, Nov. 2019.
- [79] K.-H. Yuan and P. M. Bentler. Inferences on correlation coefficients in some classes of nonnormal distributions. *Journal of Multivariate Analysis*, 72(2):230–248, 2000.
- [80] K.-H. Yuan, P. M. Bentler, and W. Zhang. The effect of skewness and kurtosis on mean and covariance structure analysis: The univariate case and its multivariate implication. *Sociological Methods & Research*, 34(2):240–258, 2005.
- [81] S. Zhang and K. Balog. Ad hoc table retrieval using semantic similarity. In *Proceedings of the 2018 World Wide Web Conference, WWW '18*, pages 1553–1562, Republic and Canton of Geneva, Switzerland, 2018. International World Wide Web Conferences Steering Committee.
- [82] S. Zhang and K. Balog. Web table extraction, retrieval, and augmentation: A survey. *ACM Transactions on Intelligent Systems and Technology (TIST)*, 11(2):1–35, 2020.
- [83] Y. Zhang and Z. G. Ives. Finding related tables in data lakes for interactive data science. In *Proceedings of the 2020 ACM SIGMOD International Conference on Management of Data*, pages 1951–1966, 2020.
- [84] E. Zhu, D. Deng, F. Nargesian, and R. J. Miller. Josie: Overlap set similarity search for finding joinable tables in data lakes. In *Proceedings of the 2019 International Conference on Management of Data, SIGMOD '19*, pages 847–864, New York, NY, USA, 2019. ACM.
- [85] E. Zhu, F. Nargesian, K. Q. Pu, and R. J. Miller. Lsh ensemble: Internet-scale domain search. *Proc. VLDB Endow.*, 9(12):1185–1196, Aug. 2016.

A APPENDIX

A.1 Proof of Theorem 1

PROOF OF THEOREM 1. Let $\mathcal{T}_{X \bowtie Y} = \langle K_{X \bowtie Y}, X_{X \bowtie Y}, Y_{X \bowtie Y} \rangle$ be the table resulting of the join between $\mathcal{T}_X = \langle K_X, X \rangle$ and $\mathcal{T}_Y = \langle K_Y, Y \rangle$. By definition, $K_{X \bowtie Y} = K_X \cap K_Y$. Let $g = h_u(h(k))$ be the composition of the hash functions h, h_u described above; g maps keys from the set $K_X \cap K_Y$ uniformly at random to $[0, 1]$. For this proof, let $g(K) = \{g(k) : k \in K\}$, $S_{X \bowtie Y}$ be the set of tuples $\{\langle k, x_k, y_k \rangle : k \in K_{X \bowtie Y}\}$ with the n smallest values $g(k) \in g(K_{X \bowtie Y})$, and $n < |K_{X \bowtie Y}|$. Notice that, because g assigns values uniformly and randomly, the set of tuples $\langle x_k, y_k \rangle \in S_{X \bowtie Y}$ is a uniform random sample of the set of tuples $\langle x_k, y_k \rangle \in \mathcal{T}_{X \bowtie Y}$.

Now consider the size- n synopses $L_{\langle K_X, X \rangle}$ and $L_{\langle K_Y, Y \rangle}$ of tables \mathcal{T}_X and \mathcal{T}_Y respectively. Let L_{K_X} and L_{K_Y} be the sets of keys from their respective synopses, i.e., $L_{K_X} = \{k_x : k_x \in L_{\langle K_X, X \rangle}\}$ and $L_{K_Y} = \{k_y : k_y \in L_{\langle K_Y, Y \rangle}\}$. Moreover, let $L_{X \bowtie Y} = \{\langle k, x_k, y_k \rangle : k \in L_{K_X} \cap L_{K_Y}\}$. Because a synopsis L always keeps the numerical values associated with their respective keys, to prove that $\langle x_k, y_k \rangle \in L_{X \bowtie Y}$ is a uniform random sample of the set of tuples $\langle x_k, y_k \rangle \in \mathcal{T}_{X \bowtie Y}$, it suffices to show that the set of keys $\{k : k \in L_{X \bowtie Y}\}$ is a uniform random sample of $K_{X \bowtie Y}$.

By definition, the set of keys $L_{K_X} \in L_{\langle K_X, X \rangle}$ (resp. $L_{K_Y} \in L_{\langle K_Y, Y \rangle}$) only contains the n keys $k \in K_X$ (resp. $k \in K_Y$) with the smallest values of $g(K_X)$ (resp. $g(K_Y)$), and the joined synopsis table $L_{X \bowtie Y}$ contains their intersection: $L_{K_X} \cap L_{K_Y}$. Thus, it is easy to see that $L_{K_X} \cap L_{K_Y} \subseteq \{k : k \in S_{X \bowtie Y}\}$ always holds. Without loss of generality, assume that $|L_{\langle K_X, X \rangle}| = |L_{\langle K_Y, Y \rangle}| = |S_{X \bowtie Y}| = n$. The best case happens when the sets of keys are equal, i.e., $L_{K_X} = L_{K_Y}$, in which case $|L_{K_X} \cap L_{K_Y}| = |S_{X \bowtie Y}|$ and $L_{K_X} \cap L_{K_Y} = \{k : k \in S_{X \bowtie Y}\}$. When $L_{K_X} \neq L_{K_Y}$, then $|L_{K_X} \cap L_{K_Y}| < |S_{X \bowtie Y}|$. Now, assume that $|L_{K_X} \cap L_{K_Y}| = 1$. Then, the single key $k \in L_{K_X} \cap L_{K_Y}$ has the smallest value of $g(k)$. The sample $S_{X \bowtie Y}$ of size 1 also contains the same key $k \in L_{K_X} \cap L_{K_Y}$. More generally, if $|L_{K_X} \cap L_{K_Y}| = m$, then the set of keys of the sample $S_{X \bowtie Y}$ of size m is equal to the set $L_{K_X} \cap L_{K_Y}$. Therefore, the set of tuples $\{\langle x_k, y_k \rangle : k \in L_{K_X} \cap L_{K_Y}\}$ induced by $L_{X \bowtie Y}$ is also a uniform random sample of $\mathcal{T}_{X \bowtie Y}$. \square